Neuropharmacology 116 (2017) 387–398

Contents lists available at ScienceDirect

Neuropharmacology

journal homepage: www.elsevier.com/locate/neuropharm

Sigma-1 receptor deficiency reduces GABAergic inhibition in the basolateral amygdala leading to LTD impairment and depressive-like behaviors

Baofeng Zhang [a, b], Ling Wang [b], Tingting Chen [b], Juan Hong [b], Sha Sha [b], Jun Wang [c, **], Hang Xiao [c], Ling Chen [a, b, *]

[a] State Key Lab of Reproductive Medicine, Nanjing Medical University, Nanjing 210029, China
[b] Department of Physiology, Nanjing Medical University, Nanjing 210029, China
[c] Department of Toxicology, School of Public Health, Nanjing Medical University, Nanjing 210029, China

ARTICLE INFO

Article history:
Received 27 August 2016
Received in revised form
17 December 2016
Accepted 16 January 2017
Available online 17 January 2017

Keywords:
Sigma-1 receptor (σ_1R)
Basolateral amygdala (BLA)
N-methyl-D-aspartate receptor (NMDAr)
$GABA_A$ receptor ($GABA_AR$)
neuronal nitric oxide synthase (nNOS)
Synaptic plasticity

ABSTRACT

Sigma-1 receptor knockout ($\sigma_1R^{-/-}$) in male mice causes depressive-like phenotype. We observed the expression of σ_1R in principal neurons of basolateral amygdala (BLA), a main region for affective regulation. The present study investigated the influence of σ_1R deficiency in BLA neurons on synaptic properties and plasticity at cortico-BLA pathway. In comparison with wild-type (WT) mice, the slopes of field excitatory postsynaptic potentials (fEPSP) were reduced in $\sigma_1R^{-/-}$ mice with the increases in paired-pulse facilitation (PPF) and paired-pulse inhibition (PPI) values. Induction of NMDA receptor (NMDAr)-dependent long-term potentiation (LTP) and NMDAr-independent long-term depression (LTD) were impaired in $\sigma_1R^{-/-}$ mice. The NMDAr NR2B phosphorylation in BLA of $\sigma_1R^{-/-}$ mice was lower than in WT mice. The coupling of nNOS to PSD-95 and nitric oxide (NO) level were reduced in BLA of $\sigma_1R^{-/-}$ mice, which were recovered by the BLA-injection of NMDAr agonist NMDA. The bath-application of NMDA in BLA slices from $\sigma_1R^{-/-}$ mice corrected the reduced fEPSP slopes and increased PPF and PPI and recovered the LTP and LTD induction, which were sensitive to nNOS inhibitor 7-NI. NO donor DETA/NO or $GABA_AR$ agonist muscimol could correct the PPI and recover LTD in $\sigma_1R^{-/-}$ mice. In addition, the BLA-injection of NMDA, DETA/NO or muscimol could relieve the depressive-like behaviors in $\sigma_1R^{-/-}$ mice. These results indicate that the σ_1R deficiency in BLA principal neurons *via* NMDAr dysfunction suppresses nNOS activity and NO production to reduce $GABA_AR$-mediated inhibition, which impairs LTD induction and causes depressive-like phenotype.

1. Introduction

Sigma-1 receptors (σ_1R) are highly expressed in the brain regions involved in emotion and neuropsychiatric disorders (Alonso et al., 2000; Hayashi and Su, 2004; Maurice et al., 2002). The σ_1R agonists are known to be a class of drugs used for the treatment of depression (Urani et al., 2001) and anxiety (Longone et al., 2011). The σ_1R knockout mice ($\sigma_1R^{-/-}$ mice) have been reported to appear depressive-like phenotype (Sabino et al., 2009; Sha et al., 2015). However, the underlying mechanisms have not yet been fully elucidated.

The activation of σ_1R potentiates the Ca2+ influx across NMDA receptor (NMDAr) by preventing small conductance Ca2+-activated K+ channels (Martina et al., 2007) or enhancing NMDAr trafficking to the plasma membrane (Pabba et al., 2014). Selective

Abbreviations: AMPAr, AMPA receptor; BCA, bicinchoninic acid; BLA, basolateral amygdala; EC, external capsule; EPSPs, excitatory postsynaptic potentials; FST, forced swim test; $GABA_AR$, $GABA_A$ receptor; HFS, high-frequency stimulation; I/O, input-output; IPI, interpulse interval; LFS, low-frequency stimulation; LTD, long-term depression; LTP, long-term potentiation; NMDAr, N-methyl-D-aspartate receptor; NO, nitric oxide; OFT, open field test; nNOS, neuronal nitric oxide synthase; PSD-95, post-synaptic density-95; PPF, paired-pulse facilitation; PPI, paired-pulse inhibition; PPR, paired-pulse ratio; TST, tail suspension test; WT mice, wild-type mice; $\sigma_1R^{-/-}$ mice, sigma-1 receptor knockout mice.

* Correspondence author. Department of Physiology, Nanjing Medical University, Tianyuan East Road 818, Nanjing, China.
** Corresponding author. Department of Toxicology, School of Public Health, Nanjing Medical University, Nanjing 210029, China.
E-mail addresses: wangjun@njmu.edu.cn (J. Wang), lingchen@njmu.edu.cn (L. Chen).

http://dx.doi.org/10.1016/j.neuropharm.2017.01.014
0028-3908/

σ_1R ligands can increase NMDA-induced norepinephrine release and neuronal firing (Monnet and Maurice, 2006). Sha et al. (2013) reported that the NMDA-activated current and phosphorylation of NMDAr NR2B subunit were reduced in hippocampal neurons of $\sigma_1R^{-/-}$ mice. In addition, the activation of σ_1R has been reported to negatively modulate GABA release (Mtchedlishvili and Kapur, 2003). However, the function of $GABA_A$ receptor ($GABA_AR$) in hippocampal neurons of $\sigma_1R^{-/-}$ mice is not altered (Sha et al., 2013). In addition, the σ_1R agonist can enhance the expression and activity of hippocampal neuronal nitric oxide synthase (nNOS) in an NMDAr-dependent manner, leading to a long-term increase in presynaptic glutamate release (Yang et al., 2011). The Ca2+ influx through the NMDAr can activate nNOS (Kiedrowski et al., 1992) through the interaction between nNOS and NMDAr that is permitted only *via* postsynaptic density protein 95 (PSD-95) (Christopherson et al., 1999). The declines in the nNOS expression and the NO production are observed in hippocampus of $\sigma_1R^{-/-}$ mice (Zhang et al., 2016).

The expression of σ_1R has been reported in the basolateral amygdala (BLA) of mice (Sanchez-Fernandez et al., 2014), one of the main brain regions for the regulation of emotional behavior. BLA contains two major types of glutamatergic principal neurons and GABAergic interneurons. The BLA principal neurons shift from regular firing to doublet or 'burst' firing during fear condition (Senn et al., 2014). A large body of evidence has established that abundant GABAergic local circuits in BLA build an excitation-inhibition cycle (Isoardi et al., 2004). The hyper-activity of BLA glutamatergic neurons is a key feature of anxiety disorders (Etkin and Wager, 2007), which is modulated by GABAergic inhibition (Spampanato et al., 2011; Zhou et al., 2011b). The plasticity of glutamatergic synapses in BLA, long-term potentiation (LTP) and long-term depression (LTD), is regulated by the Ca2+ influx from NR2B-containing NMDAr (Paoletti et al., 2013; Schroeder and Shinnick-Gallagher, 2004) and the GABAergic inhibition (Shaban et al., 2006). The production of LTP underlies the acquisition and consolidation of fear memories (Goosens and Maren, 2002), while LTD induction is thought to facilitate the extinction of learned fear (Dalton et al., 2012). Therefore, it is of great interest to investigate whether the σ_1R deficiency affects the synaptic function and plasticity in BLA.

In the present study, we used adult male $\sigma_1R^{-/-}$ mice and investigated the influence of the σ_1R deficiency on basal synaptic properties and plasticity in BLA. To explore the underlying mechanisms, we further examined the phosphorylation of NMDAr NR2B, the interaction of nNOS and PSD-95, and the NO production. Finally, we analyzed the causal link between the synaptic plasticity in BLA and the depressive-like phenotype in $\sigma_1R^{-/-}$ mice. Our results indicate that the σ_1R deficiency in BLA principal neurons reduces the $GABA_A$R-mediated inhibition to impair LTD induction and cause depressive-like phenotype.

2. Material and methods

2.1. Animals

All animal experiments were approved by the Institutional Animal Care and Ethical Committee of the Nanjing Medical University and were performed in accordance with the Laboratory Animal Research Institute for Experimental Animals guidelines. Animals were housed in plastic cages at 23 ± 2 °C and 55% relative humidity with a 12:12 h light/dark cycle in the Animal Research Center of Nanjing University. Water and food were given ad libitum. All efforts were made to minimize animal suffering and to reduce the number of animals used. The σ_1R knockout ($\sigma_1R^{-/-}$) mice were generated and characterized as described previously (Sabino et al., 2009). In this study, 12-week-old male $\sigma_1R^{-/-}$ mice and wild-type (WT) littermates were used at the beginning of the experiment. Each experiment was performed by two experimenters who were blinded to the experimental groups.

2.2. Behavioral examination

A single cohort of animals was used for the following test sequence: open-field test → forced swim test → tail suspension test (Zhou et al., 2011a). All behavioral data were captured by a video-monitor and analyzed using TopScan Lite 2.0 (Clever Sys., Reston, VA).

Open field test (OFT) was performed in a cuboid plexiglass box (60 cm × 60 cm × 40 cm) with the gray floor divided into 16 equal squares. The central zone was defined as the central 4 squares (30 cm × 30 cm). Each mouse was placed in a corner of the arena and allowed to freely explore for 6 min. Following parameters were evaluated: total distance traveled (mm/6 min) and the time spent in the center region.

Tail suspension test (TST) was performed by suspending the mice tail using adhesive tape to a rod 60 cm above the floor. Trials were conducted for 6 min to record the duration of immobility.

Forced swim test (FST) was performed by placing mice in plastic cylinders (diameter 12 cm, height 24 cm) filled with water (23–25 °C) to a height of 20 cm. Total duration of immobility during a 6 min test was scored. The mouse was considered to be immobile when it stopped struggling and moved only to remain floating in the water, keeping its head above water.

2.3. Morphologic examination

Animals were deeply anesthetized with chloral hydrate (400 mg/kg, i.p.) and cardinally perfused with cold PBS followed by 4% paraformaldehyde. Brains were removed and processed for paraffin embedding. Coronal sections (5 μm in thickness) were placed in gelatine-coated slides, and then were stained with toluidine blue. BLA was observed using a conventional lightmicroscope (Olympus DP70) with 10 × objective. For σ_1R immunohistochemistry staining, the sections were treated with 5% normal goat serum and then incubated in a mouse anti-σ_1R (1:250; Santa Cruz, CA, USA) at 4 °C overnight. After PBS rinses, the sections were incubated in biotin-labeled donkey anti-mouse IgG antibody (1:400; Santa Cruz) for 2 h. Immunoreactivities were visualized by avidin-biotin horseradish peroxidase complex (ABC Elite; Vector Laboratories) using 3,3'-diaminobenzidine as the chromogen. The σ_1R positive cells were observed using a conventional light microscope (40 × objective, DP70; Olympus).

2.4. Slice preparation and BLA collection

Mice were decapitated under deep anesthesia with isoflurane and the brains were rapidly removed. The coronal brain slices (400–600 μm in thickness) were cut using a vibrating microtome (Microslicer DTK 1500, Dousaka EM Co, Kyoto, Japan) in ice-cold oxygenated (95% O_2/5% CO_2) cutting solution composed of (in mM) 94 sucrose, 30 NaCl, 4.5 KCl, 1.0 MgCl2, 26 NaHCO3, 1.2 NaH2PO4, and 10 D-glucose, pH 7.4. The slices (600 μm) were incubated in a rest chamber containing fresh oxygenated ACSF at 30 ± 1 °C for recovery from damage. After 60 min of recovery, the regions containing the BLA (shown in Fig. 1C) were rapidly harvested using a 15-gauge needle (inner diameter 1.5 mm) for NO examination, co-immunoprecipitation, Western Blotting and RT-PCR.

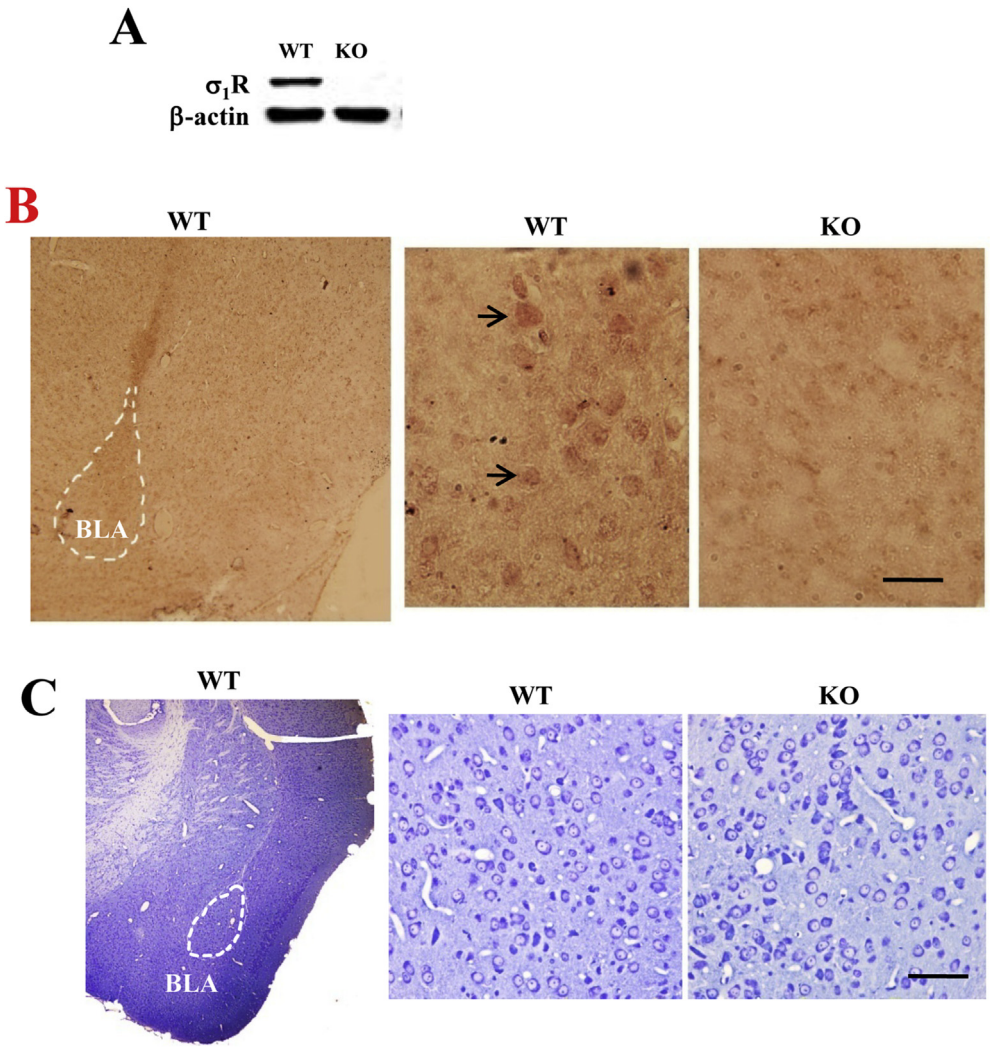

Fig. 1. Expression of σ_1R in BLA principal neurons. (**A**) Representative blots of σ_1R protein in BLA of WT mice (WT) and $\sigma_1R^{-/-}$ mice (KO). (**B**) Representative photomicrograph of a σ_1R-immunohistochemical staining and σ_1R positive principal neurons (arrows) in BLA. The BLA area is indicated by a white broken line. Scale bars = 25 μm. (**C**) A Representative images of BLA stained with toluidine blue in WT mice and $\sigma_1R^{-/-}$ mice. Scale bars = 50 μm.

2.5. Field potential recording

The slices (400 μm) were transferred to a recording chamber and perfused continually with oxygenated artificial cerebrospinal fluid (ACSF) composed of (in mM) 124 NaCl, 2 CaCl2, 4.5 KCl, 1 MgCl2, 26 NaHCO3, 1.2 NaH2PO4, and 10 D-glucose (pH value of ACSF was adjusted to 7.4) at 30 ± 1 °C. A bipolar tungsten electrode was placed outside BLA to stimulate the external capsule (EC) fibers from the cortex. The constant current pulses (pulse width: 100 ms; frequency: 0.05 Hz) were supplied by a stimulator (SEN-3301, Nihon Kohden, Japan). Field excitatory postsynaptic potentials (fEPSPs) were recorded from BLA by a 5 MΩ resistance glass microelectrode that was filled with 2 M NaCl, and connected to a neutralized, high input-impedance preamplifier with a high-pass filter at 5 kHz. Signals were amplified with the use of a differential AC amplifier (A-M Systems, model 1700, Seattle, WA) and were digitized and saved using the pCLAMP system (Axon Instrument Inc., CA, USA). The fEPSPs were digitized and saved using a pCLAMP system (Axon). Generally, the test stimulus was set at approximately 50% of the maximum stimulus intensity that evoked a saturated fEPSP in each slice. Following parameters were evaluated: (1) input/output function was assessed by averaging the stimulus intensity from 0.1 mA to 1.1 mA; (2) paired-pulse facilitation (PPF) was induced by paired-pulse simulation with interpulse interval (IPI) of 25–100 ms; (3) paired-pulse inhibition (PPI) was induced by paired-pulse simulation with an IPI of 25 ms; (4) LTP was induced using a protocol of high-frequency stimulation (HFS), which consisted of five trains of stimulation (100 Hz for 1 s) at 20 s intervals (Li and Rainnie, 2014); (5) LTD was induced by delivering low-frequency stimulation (LFS, 1 Hz 15 min) (Li and Rainnie, 2014). Paired-pulse ratio (PPR) was calculated with the following formula: ($fEPSP_2/fEPSP_1$) × 100, where $fEPSP_1$ and $fEPSP_2$ represent the fEPSP slopes evoked by the first and second stimulation, respectively. After delivering HFS or LFS, the fEPSP slopes were recorded for over 60 min. LTP or LTD was determined if the fEPSP slopes were greater or lower than 20% of baseline at 55–60 min after delivering HFS or LFS.

2.6. Nitric oxide examination

NO was estimated as a formed nitrite (NO2-) using a Griess reagent assay for nitrite according to the manufacturer's protocol (Promega, Madison, WI, USA) (Chae et al., 2004). BLA was homogenized by sonication in lysis buffer, and then centrifuged for

5 min at 12,000 × g at 4 °C. The supernatant (30 μl) was added with sulfanilamide solution (1% sulfanilamide in 5% phosphoric acid, 50 μl). After the incubation for 10 min at room temperature, the sample was again added with 0.1% N-1-napthylethylenediamine dihydrochloride (50 μl). The absorbance was measured at 540 nm using a microplate reader within 30 min. The nitrite content was calculated based on a standard curve constructed with $NaNO_2$.

2.7. Coimmunoprecipitation and western blotting

Tissues of BLA were homogenized in 1% Nonidet P-40 lysis buffer containing 50 mM Tris, 150 mM NaCl, 0.02% NaN3, and complete protease inhibitors (Roche). The homogenates were centrifuged for 15 min at 12,000 r.p.m. (Thermo Scientific) and the supernatants were collected. Protein concentrations were determined using a bicinchoninic acid (BCA) protein assay kit (Pierce).

For co-immunoprecipitation (co-IP), the protein (500 μg) were pre-incubated for 1 h with 40 μl protein A/G-Sepharose (GE Healthcare, Sweden) and then centrifuged at 12,000 × g to remove any nonspecific binding to protein A/G. The supernatant was incubated with 2 μg mouse anti-nNOS (1:1000; Chemicon, USA, CA, USA) overnight at 4 °C and then with protein A/G-Sepharose (40 μl) overnight at 4 °C. Samples were centrifuged at 12,000 × g, and the pellets were washed five times with homogenization buffer (Yang et al., 2010). Bound proteins were eluted by adding sample buffer (20 μl) and boiling at 100 °C for 5 min. Samples were finally centrifuged and supernatants were analyzed by Western blotting.

For Western blotting, 20 μg of total protein (boiled) or immunoprecipitated protein was separated by 8% acrylamide denaturing gels (SDS-PAGE) and transferred to membranes. The membranes were incubated with rabbit monoclonal anti-phospho-NR2B (1:1000; Millipore, MA, USA), anti-phospho-NR2A antibody (1:1000; Abcam, Cambridge, UK), mouse anti-nNOS (1:1000; Chemicon, USA, CA, USA), mouse anti-σ_1R (1:500; Santa Cruz, CA, USA), anti-PSD-95 (1:1000, Cell Signaling, MA, USA) and anti-calmodulin (1:1000; Cell Signaling). After TBST buffer rinses, the membranes were incubated with horse radish peroxidase-labeled goat anti-rabbit antibody (1:5000; Santa Cruz, CA) and developed using an enhanced chemiluminescence detection kit (Millipore). Following visualization, the blots were stripped by incubation in stripping buffer (Restore; Pierce) for 15 min; and then incubated with antibodies of anti-NR2B and anti-NR2A (1:1000; Millipore), anti-β-actin (1:1000, Cell Signaling). Western blot bands were scanned and analyzed using the Image J analysis software package (NIH). The densitometric value of phosphorylated protein normalized by total protein was normalized again by the control level. Each experiment was performed in quadruplicate using tissue from 8 mice per group.

2.8. Reverse transcription-polymerase chain reaction (RT-PCR)

Total RNA was isolated from the BLA with TRIzol reagent (Invitrogen, Camarillo, CA) and reverse-transcribed into cDNA using a Prime Script RT reagent kit (Takara, China) for quantitative PCR (ABI Step One Plus, Foster City, CA) in the presence of a fluorescent dye (SYBR Green I; Takara, China). PCR was performed in triplicate with 10 μl template DNA per well and run for 40 cycles. The relative expression of genes was determined using the 2-ΔΔct method with normalization to GAPDH and β-actin in each sample. The results were averaged from four sets of independent experiments. The primer sets used for GluR1, GluR2, NR1, NR2B, NR2A, $GABA_AR$-α4, $GABA_AR$-δ, GAPDH and β-actin were designed according to earlier publications (Wright et al., 2014; Zhou et al., 2016).

2.9. Administration of drugs

NMDAr agonist NMDA and antagonist MK801, AMPAr antagonist CNQX, $GABA_AR$ agonist muscimol and antagonist bicuculline, NO donor DETA/NONOate (DETA/NO) and nNOS inhibitor 7-nitroindazole (7-NI) were purchased from Sigma-Aldrich (St. Louis, MO, USA). CNQX, NMDA, muscimol, bicuculline, DETA/NO and 7-NI were dissolved in distilled water for stock solutions. For *in vitro* experiment, the slices were incubated in ACSF containing NMDA (10 μM), the AMPAr antagonist CNQX (10 μM), the NO donor DETA/NO (3 mM), the nNOS inhibitor 7-NI (5 μM), the $GABA_AR$ agonist muscimol (10 μM) or antagonist bicuculine (10 μM) for 30 min (Pose et al., 2014; Yang et al., 2011; Zhou et al., 2011b). For *in vivo* experiment, the mice were anesthetized with chloral hydrate (400 mg/kg, i.p.) and placed into a stereotaxic instrument (Stoelting, Wood Dale, IL). The scalp was incised and a small hole (2 mm diameter) was drilled in the skull using a dental drill. Guide cannulas (26-Gauge, Plastics One, Roanoke, VA) were implanted into the bilateral BLA (1.4 mm posterior, ±3.0 mm lateral, and 4.8 mm ventral to bregma). On day 3 after surgery, the dummy cannulas were removed from the guide cannula, and then replaced by infusion cannulas (30 Gauge). The infusion cannula was connected by polyethylene tubing (PE 10; Becton Dickinson, Sparks, MD) with a stepper-motorized micro-syringe (Stoelting, Wood Dale, IL, USA). ACSF containing Muscimol (4 nmol), NMDA (5 nmol), DETA/NO (10 nmol) and 7-NI (10 nmol) were infused in a volume of 0.25 μl/side (Fendt et al., 2003; Hu et al., 2012; Zhou et al., 2011b). After the behavioral tests, 2% Evans Blue (0.05 ml) was injected. The mice were killed by an overdose of chloral hydrate, and coronal sections (100 μm) were cut using a cryostat to validate the injection-site.

2.10. Data analysis

Data were retrieved and processed with the software Microcal Origin 6.1. The group data were expressed as the mean ± standard error (SE). Experimental results were compared among treatment groups by ANOVAs followed by Bonferroni's posthoc test or *t*-test. Statistical analyses were performed using State7 software (STATA Corporation, USA). $P < 0.05$ was considered statistically significant.

3. Results

3.1. Expression of σ_1R in BLA principal neurons

Consistent with the report by Sanchez-Fernandez et al. (2014), the σ_1R protein at approximately 28 kDa was observed in BLA of WT mice, but not in $\sigma_1R^{-/-}$ mice (Fig. 1A). Using immunohistochemical staining, we observed the σ_1R positive neurons in the BLA of WT mice (Fig. 1B). These σ_1R positive neurons showed a large triangle shaped soma, which are called BLA pyramidal neurons or BLA principal neurons (Klenowski et al., 2015). Although there was not the σ_1R positive neurons in BLA of $\sigma_1R^{-/-}$ mice, the density of BLA principal neurons was not altered compared to WT mice (Fig. 1C).

3.2. Influence σ_1R deficiency on synaptic properties in BLA

By stimulating external capsule (EC) fibers in the slices obtained from WT mice or $\sigma_1R^{-/-}$ mice (Fig. 2A), we recorded a field excitatory postsynaptic potential (fEPSP) in BLA (Fig. 2B), termed "EC-BLA synaptic transmission". To evaluate the basal properties of the EC-BLA synapses, an input-output curve was built by plotting fEPSP slopes against stimulation intensities (SI) from 0.1 mA to 1.1 mA. The fEPSP slopes (0.3–0.7 mA/SI) in $\sigma_1R^{-/-}$ mice were lower than

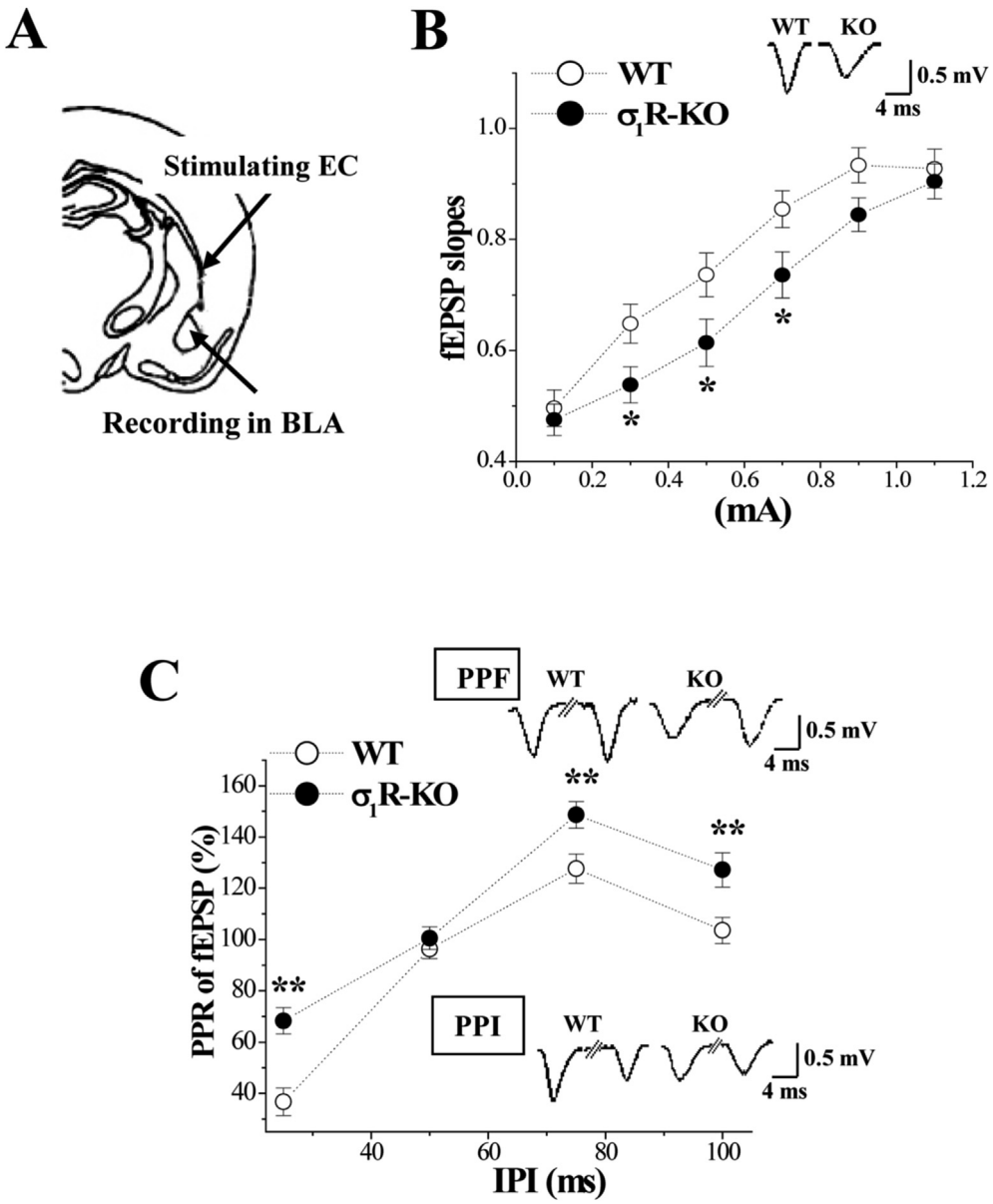

Fig. 2. Influence σ_1R deficiency on synaptic properties in BLA. (**A**) Schematic illustrating spots of stimulating external capsule (EC) fibers and the field excitatory post-synaptic potentials (fEPSPs) in the BLA, termed EC-BLA synaptic transmission. (**B**) Input-output (I/O) curve. Each point represents the group mean value of fEPSP slopes against stimulus intensity from 0.1 mA to 1.1 mA in the BLA of WT mice and $\sigma_1R^{-/-}$ mice. *$P < 0.05$ *vs*. WT mice (two-way ANOVA). Representative sampling traces of fEPSP slopes at 0.5 mA stimulus intensity in WT mice (WT) and $\sigma_1R^{-/-}$ mice (KO). (**C**) Paired-pulse facilitation (PPF) and paired-pulse inhibition (PPI) of fEPSP in the BLA. Paired-pulse ratio (PPR, %) of fEPSP slopes was plotted against various interpulse intervals (IPIs) ranging from 25 ms to 100 ms. Typical traces evoked with IPI of 75 ms (PPF, upper panel) and 25 ms (PPI, under panel) in WT mice (WT) and $\sigma_1R^{-/-}$ mice (KO). **$P < 0.01$ *vs*. WT mice (two-way ANOVA).

those in WT mice ($P < 0.05$, n = 10 slices/5 mice). The paired-pulse facilitation (PPF) of fEPSP slopes was elicited by two successive stimulations (0.5 mA/SI) with interpulse interval (IPI) at 50–100 ms to evaluate the capability of presynaptic glutamate release. As shown in Fig. 1C, the values of PPF (75–100 ms/IPI) in $\sigma_1R^{-/-}$ mice were larger than those in WT mice ($P < 0.01$, n = 10). The paired-pulse inhibition (PPI) is considered to depend on a $GABA_AR$-mediated inhibitory postsynaptic potential in BLA (Delaney and Sah, 2001), we examined the PPI of fEPSP slopes by delivering paired-pulse stimulation (0.5 mA/SI) with IPI at 25 ms. The results showed that the PPI value in $\sigma_1R^{-/-}$ mice was increased compared to WT mice ($P < 0.01$, n = 10; Fig. 1C). These results indicate that σ_1R deficiency in BLA neurons attenuates the capability of presynaptic glutamate release and $GABA_AR$-mediated inhibition.

3.3. Influence of σ_1R deficiency on NMDAr, nNOS and NO in BLA

To explore the mechanisms underlying synaptic dysfunction in the BLA of $\sigma_1R^{-/-}$ mice, we examined the expression of AMPAr, NMDAr and $GABA_AR$. The analysis of RT-PCR showed that the levels of *GluR1*, *GluR2*, *NR1*, *NR2B*, *NR2A*, *$GABA_AR$-α4* and *$GABA_AR$-δ* mNRA in BLA had no significant difference between $\sigma_1R^{-/-}$ mice and WT mice ($P > 0.05$, n = 8 mice; Fig. 3A). The level of the NMDAr NR2B phosphorylation (phosphor-NR2B) in BLA of $\sigma_1R^{-/-}$ mice was lower than that in WT mice ($P < 0.01$, n = 8; Fig. 3B), but the NR2A phosphorylation (phosphor-NR2A) did not differ from WT mice ($P > 0.05$, n = 8; Fig. 3C).

In the BLA principal neurons, NO has been described to modulate the activity of glutamatergic synapses (Schafe et al., 2005).

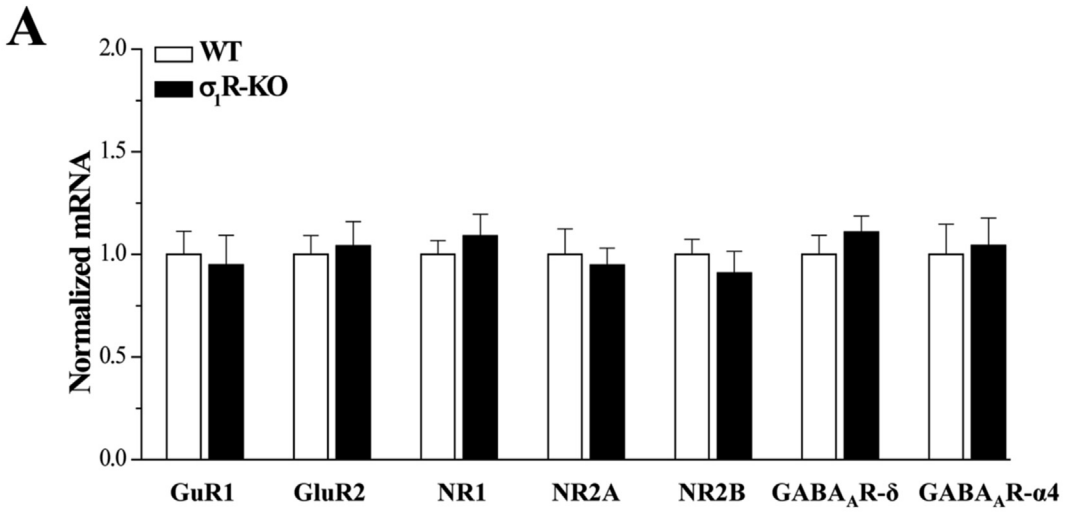
A
WT
σ1R-KO
Normalized mRNA
2.0
1.5
1.0
0.5
0.0
GuR1
GluR2
NR1
NR2A
NR2B
GABAAR-δ
GABAAR-α4

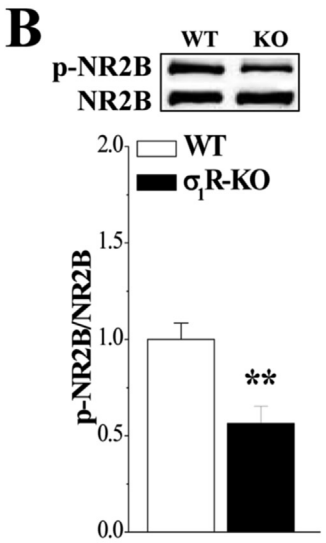
B
WT
KO
p-NR2B
NR2B
WT
σ1R-KO
p-NR2B/NR2B
2.0
1.5
1.0
0.5
0.0
**

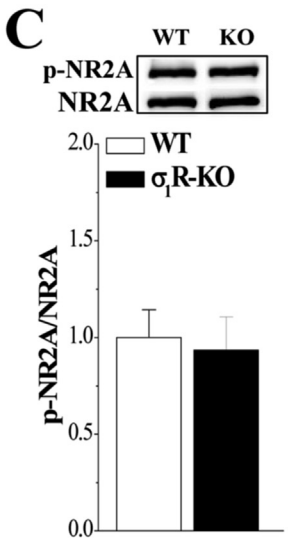
C
WT
KO
p-NR2A
NR2A
WT
σ1R-KO
p-NR2A/NR2A
2.0
1.5
1.0
0.5
0.0

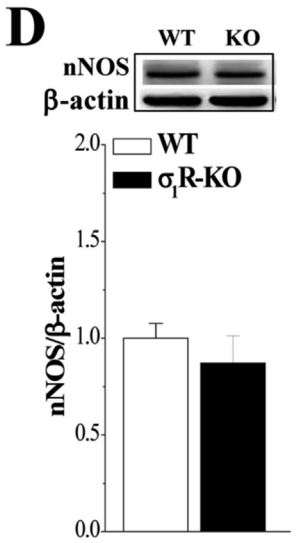
D
WT
KO
nNOS
β-actin
WT
σ1R-KO
nNOS/β-actin
2.0
1.5
1.0
0.5
0.0

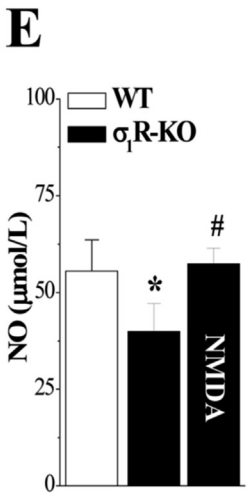
E
WT
σ1R-KO
NO (μmol/L)
100
75
50
25
0
*
#
NMDA

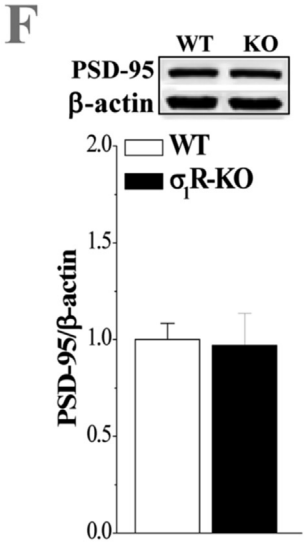
F
WT
KO
PSD-95
β-actin
WT
σ1R-KO
PSD-95/β-actin
2.0
1.5
1.0
0.5
0.0

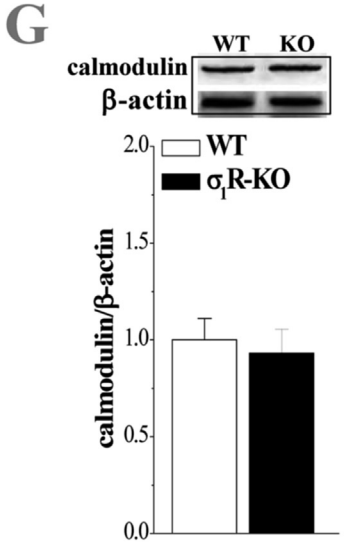
G
WT
KO
calmodulin
β-actin
WT
σ1R-KO
calmodulin/β-actin
2.0
1.5
1.0
0.5
0.0

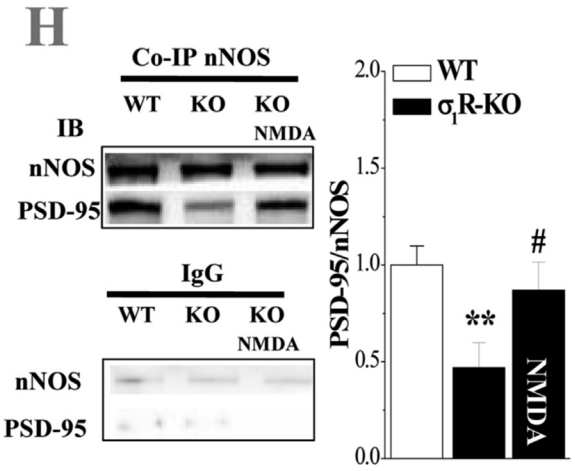
H
Co-IP nNOS
WT
KO
KO
NMDA
IB
nNOS
PSD-95
IgG
WT
KO
KO
NMDA
nNOS
PSD-95
WT
σ1R-KO
PSD-95/nNOS
2.0
1.5
1.0
0.5
0.0
**
#
NMDA

Neuronal NO synthase (nNOS) is the predominant source of NO in neurons (Boehning and Snyder, 2003). The results of western blots revealed that $\sigma_1R^{-/-}$ mice had a tendency to reduce the level of nNOS expression in BLA, but the group comparison with WT mice failed to reach significance ($P > 0.05$, n = 8; Fig. 3D). Importantly, we observed a slight but significant decrease in the NO level in BLA of $\sigma_1R^{-/-}$ mice ($P < 0.05$, n = 8; Fig. 3E), which was corrected by the BLA-injection of the NMDAr agonist NMDA ($P < 0.05$, n = 8).

The activity of nNOS is primarily regulated by its interaction with the Ca2+-calmodulin complex, which depends on the Ca2+ influx of NMDAr increases (Hisatsune et al., 1997). The coupling of nNOS to NMDAr involves the scaffolding protein PSD-95 (Christopherson et al., 1999). The levels of NMDAr ($P > 0.05$, n = 8; Fig. 3B), PSD-95 ($P > 0.05$, n = 8; Fig. 3F) and calmodulin proteins ($P > 0.05$, n = 8; Fig. 3G) in BLA of $\sigma_1R^{-/-}$ mice had no difference from WT. To test whether the reduced NMDAr activity in $\sigma_1R^{-/-}$ mice affects the interaction of nNOS and NMDAr, further experiment was designed to examine the co-immunoprecipitation of nNOS with PSD-95. The results showed that the interaction of nNOS with PSD-95 in BLA of $\sigma_1R^{-/-}$ mice was significantly reduced in comparison with WT mice ($P < 0.01$, n = 8; Fig. 3H), which could be corrected by the BLA-injection of NMDA ($P < 0.05$, n = 8). These results indicate that σ_1R deficiency in BLA neurons *via* reduced activity of NMDAr attenuates the nNOS activation and NO production.

3.4. Involvement of reduced NO in synaptic dysfunction of BLA

To test the involvement of reduced NO level in synaptic dysfunction in BLA of $\sigma_1R^{-/-}$ mice, the BLA slices were treated with the path-application of NMDA (10 μM), the AMPAr antagonist CNQX (10 μM), the NO donor DETA/NO (3 mM), the nNOS inhibitor 7-NI (5 μM), the $GABA_AR$ agonist muscimol (10 μM) or antagonist bicuculine (10 μM) for 30 min. The EC-BLA synaptic transmission in WT mice was blocked by CNQX ($P < 0.01$, n = 10 slices/5 mice; Fig. 4A). The application of NMDA in $\sigma_1R^{-/-}$ mice corrected the reduced fEPSP slope ($P < 0.05$, n = 10) and the increased PPF ($P < 0.01$, n = 10; Fig. 4B), which was blocked by 7-NI (slopes: $P < 0.05$, n = 10; PPF: $P < 0.01$, n = 10) and could be mimicked by DETA/NO (slopes: $P < 0.05$, n = 10; PPF: $P < 0.01$, n = 10). The application of NMDA in $\sigma_1R^{-/-}$ mice was able to correct the increased PPI ($P < 0.01$, n = 10; Fig. 4C), which was sensitive to 7-NI ($P < 0.01$, n = 10). The increased PPI in $\sigma_1R^{-/-}$ mice was corrected by DETA/NO ($P < 0.01$, n = 10). In addition, the application of bicuculine caused the increase in the PPI value in WT mice ($P < 0.01$, n = 10), but not in $\sigma_1R^{-/-}$ mice ($P > 0.05$, n = 10). However, the addition of bicuculine could prevent the NMDA- or DETA/NO-corrected PPI in $\sigma_1R^{-/-}$ mice ($P < 0.01$, n = 10), indicating that bicuculine can increase the PPI value in $\sigma_1R^{-/-}$ mice when the increased PPI was corrected by NMDA or DETA/NO. In addition, the application of bicuculine in WT mice caused a significant increase in the fEPSP slopes ($P < 0.01$, n = 10 slices/5 mice; Fig. 4D), but in the $\sigma_1R^{-/-}$ slices was hardly altered the fEPSP slopes ($P > 0.05$, n = 10). The application of muscimol reduced the fEPSP slopes in WT mice ($P < 0.05$, n = 10) and $\sigma_1R^{-/-}$ mice ($P < 0.01$, n = 10). These results indicate that the σ_1R deficiency through reducing NO attenuates presynaptic glutamate release and the $GABA_AR$-mediated inhibition.

3.5. Influence σ_1R deficiency on synaptic plasticity in BLA

The Ca2+ influx of NMDAr and the GABAergic inhibition can modulate the inductions of EC-BLA synaptic LTP and LTD. The application of high-frequency stimulation (HFS) in WT mice induced an approximately 35% increase in the fEPSP slopes for over 60 min (n = 10 slices/5 mice; Fig. 5A), indicative "LTP". The induction of LTP was blocked by the application of 10 μM MK801 (n = 10). In contrast, the same HFS protocol could not induce the LTP in $\sigma_1R^{-/-}$ mice (n = 10; Fig. 5B), which was rescued by the application of NMDA (n = 10). The effect of NMDA on the LTP induction was sensitive to 7-NI (n = 10; Fig. 5C), whereas the application of alone DETA/NO could not recover the LTP induction in $\sigma_1R^{-/-}$ mice (n = 10). In WT mice, the fEPSP slopes were decreased by delivering low-frequency stimulation (LFS) for over 60 min (n = 10; Fig. 5D), indicative "LTD". The induction of LTD was insensitive to MK801 (n = 10), whereas was blocked by the application of bicuculine (n = 10; Fig. 5E). In $\sigma_1R^{-/-}$ mice, the same LFS protocol did not induce a stable decrease in the fEPSP slopes (n = 10; Fig. 5F), which could be rescued by the application of muscimol (n = 10). The application of NMDA perfectly recovered the induction of LTD in $\sigma_1R^{-/-}$ mice (n = 10; Fig. 5G), which was sensitive to 7-NI (n = 10). Moreover, the induction of LTD in $\sigma_1R^{-/-}$ mice was rescued by DETA/NO (n = 10; Fig. 5H), which was blocked by bicuculine (n = 10). These results indicate that the σ_1R deficiency impairs the LTD induction *via* the reduction of $GABA_AR$-mediated inhibition.

3.6. Relation of impaired LTD in BLA of $\sigma_1R^{-/-}$ mice with depressive-like behaviors

Behavioral experiments suggest that the EC-BLA synaptic plasticity is involved in the storage of long-term fear memories. Spontaneous activity, anxiety- and depression-like behaviors were further examined by open-field test (OFT), forced swim test (FST) and tail suspension test (TST). As shown in Fig. 6A, the distance traveled in OFT had any difference between WT mice and $\sigma_1R^{-/-}$ mice ($P > 0.05$, n = 10 mice). Although $\sigma_1R^{-/-}$ mice had a tendency to reduce the time spent in the central partition of the arena, the group when compared with WT mice failed to reach the significance ($P > 0.05$, n = 10; Fig. 6B). The application of muscimol or NMDA in $\sigma_1R^{-/-}$ mice failed to alter the distance traveled ($P > 0.05$, n = 10 mice) or the time spent in the central partition ($P > 0.05$, n = 10 mice). In comparison with WT mice, the prolongation of immobility time in FST ($P < 0.01$, n = 10 mice; Fig. 6C) and TST ($P < 0.01$, n = 10; Fig. 6D) was observed in $\sigma_1R^{-/-}$ mice, which could be improved by the BLA-injction of muscimol (FST: $P < 0.01$; TST: $P < 0.01$, n = 10) or DETA/NO (FST: $P < 0.05$; TST: $P < 0.01$, n = 10) for 3 days. The BLA-injection of NMDA for 3 days in $\sigma_1R^{-/-}$ mice could relieve the depressive-like behaviors (FST: $P < 0.01$; TST: $P < 0.01$, n = 10), which was sensitive to 7-NI (FST: $P < 0.01$; TST: $P < 0.01$, n = 10). These results indicate that the LTD impairment in $\sigma_1R^{-/-}$ mice is involved in the production of depressive-like phenotype.

Fig. 3. Influence of σ_1R deficiency on NMDAr, nNOS and NO in BLA. (**A**) Levels of *GluR1*, *GluR2*, *NR1*, *NR2B*, *NR2A*, *$GABA_AR$-α4* and *$GABA_AR$-δ* mRNA in BLA of WT mice and $\sigma_1R^{-/-}$ mice. (**B&C**) Bar graphs show levels of phosphor-NR2B and phosphor-NR2A in BLA of WT mice (WT) and $\sigma_1R^{-/-}$ mice (KO). Densitometric values of phosphorylated proteins normalized by total protein were normalized by control levels obtained from WT mice. $^{**}P < 0.01$ *vs.* WT mice. (**D**) Levels of nNOS normalized by β-actin in BLA. (**E**) Levels of NO in BLA of WT mice, $\sigma_1R^{-/-}$ mice and NMDA-treated $\sigma_1R^{-/-}$ mice. $^{*}P < 0.05$ *vs.* WT mice; #$P < 0.05$ *vs.* $\sigma_1R^{-/-}$ mice. (**F&G**) Levels of PSD-95 and calmodulin proteins normalized by β-actin in BLA. (**H**) Representative blots from a coimmunoprecipitate experiment investigating the interaction between NOS and PSD-95 in BLA. Bar graph shows the quantitative analysis of PSD-95/nNOS association in WT mice, $\sigma_1R^{-/-}$ mice and NMDA-treated $\sigma_1R^{-/-}$ mice. $^{**}P < 0.01$ *vs.* WT mice; #$P < 0.05$ *vs.* $\sigma_1R^{-/-}$ mice.

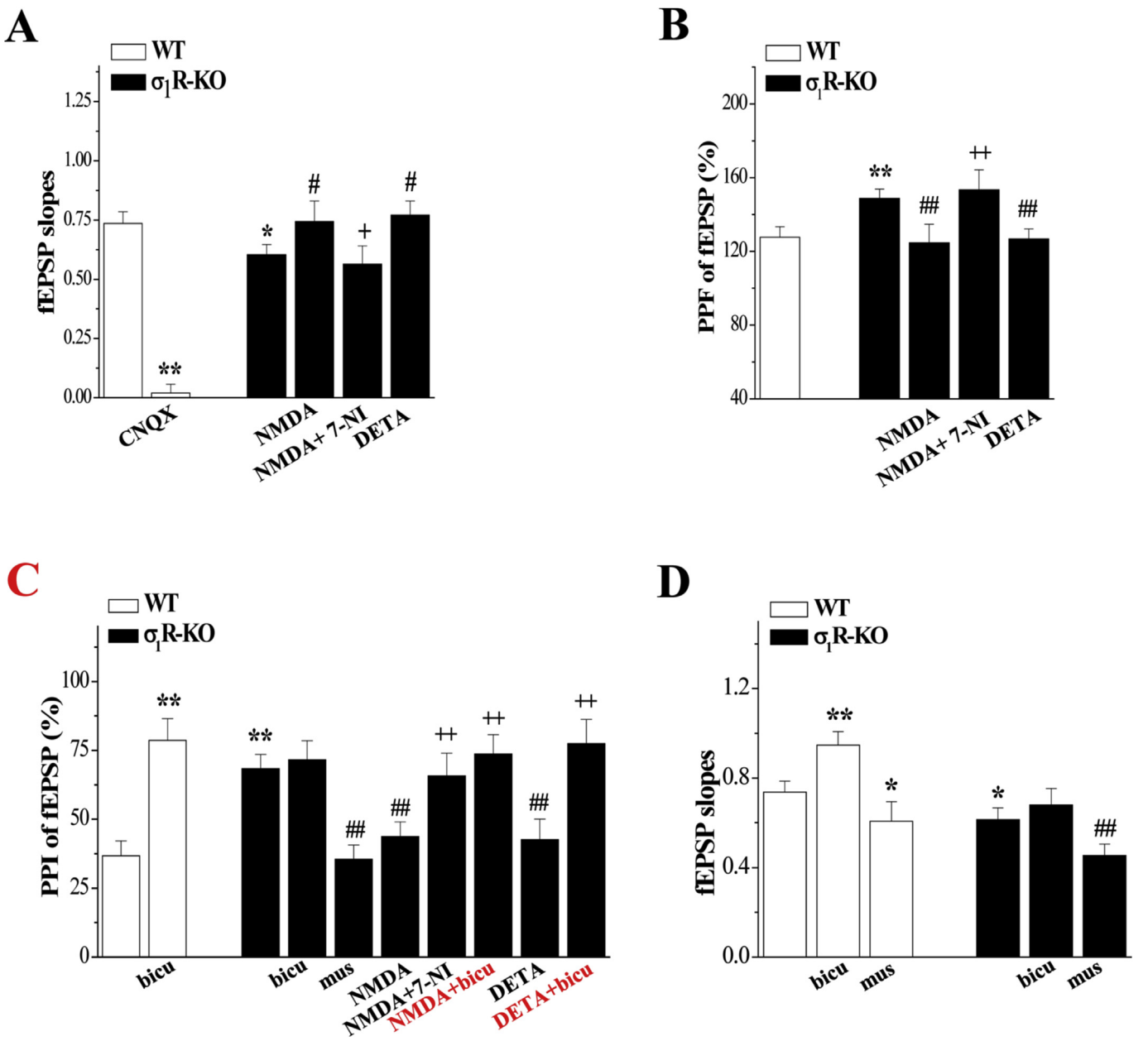

Fig. 4. Involvement of reduced NO in synaptic dysfunction of BLA. (**A&B**) Bar graphs show the mean of fEPSP slopes (0.5 mA/SI) or PPF (75 ms/IPI) in WT mice or $\sigma_1R^{-/-}$ mice. The slices were treated with the bath-application of CNQX (10 μM), NMDA (10 μM), 7-NI (5 μM) and DETA/NO (3 mM). $^{*}P < 0.05$ and $^{**}P < 0.01$ *vs.* WT mice; $\#P < 0.05$ and $\#\#P < 0.01$ *vs.* $\sigma_1R^{-/-}$ mice; $+P < 0.05$ and $++P < 0.01$ *vs.* $\sigma_1R^{-/-}$ mice treated with NMDA. (**C**) Bar graph shows the PPI (25 ms/IPI) in WT mice or $\sigma_1R^{-/-}$ mice. The slices were treated with the bath-application of bicuculine, muscimol, NMDA, 7-NI or DETA/NO. $^{**}P < 0.01$ *vs.* WT mice; $\#\#P < 0.01$ *vs.* $\sigma_1R^{-/-}$ mice; $++P < 0.01$ *vs.* $\sigma_1R^{-/-}$ mice treated with NMDA (two-way ANOVA). (**D**) Bars represent the mean of fEPSP slopes (0.5 mA/SI) in WT mice or $\sigma_1R^{-/-}$ mice. The slices were treated with the bath-application of bicuculine (bicu, 10 μM) or muscimol (mus, 10 μM). $^{*}P < 0.05$ and $^{**}P < 0.01$ *vs.* WT mice; $\#\#P < 0.01$ *vs.* $\sigma_1R^{-/-}$ mice (two-way ANOVA).

4. Discussion

Using the model of adult σ_1R knockout mouse, the present study provided the evidence that the σ_1R deficiency in BLA principal neurons decreases the $GABA_AR$-mediated inhibition to impair LTD induction, leading to the production of depressive-like phenotype.

The fEPSP slopes at the EC-BLA synapses were decreased in $\sigma_1R^{-/-}$ mice compared to WT mice, which were associated with an increase in the PPF value rather than the change in the level of AMPAr expression, indicating that the σ_1R deficiency in BLA principal neurons reduces the probability of presynaptic glutamate release. The activation of σ_1R by the σ_1R agonist or neurosteroid pregnenolone sulfate (PREGS) in cultured hippocampal neurons has been reported to increase spontaneous glutamate release (Meyer et al., 2002; Schiess and Partridge, 2005). Further study found that PREGS caused a short-term increase in the probability of hippocampal glutamate release in immature synapses (Mameli et al., 2005). This effect is likely mediated by presynaptic NMDAr containing the NR2D subunit that is transiently expressed during development. By contrast, the PREGS-induced long-term increase of glutamate release in adult rats requires the activation of post-synaptic NMDAr containing NR2B subunits (Mameli et al., 2005). An electrophysiological analysis has demonstrated the dysfunction of NMDAr in hippocampal pyramidal neurons of $\sigma_1R^{-/-}$ mice

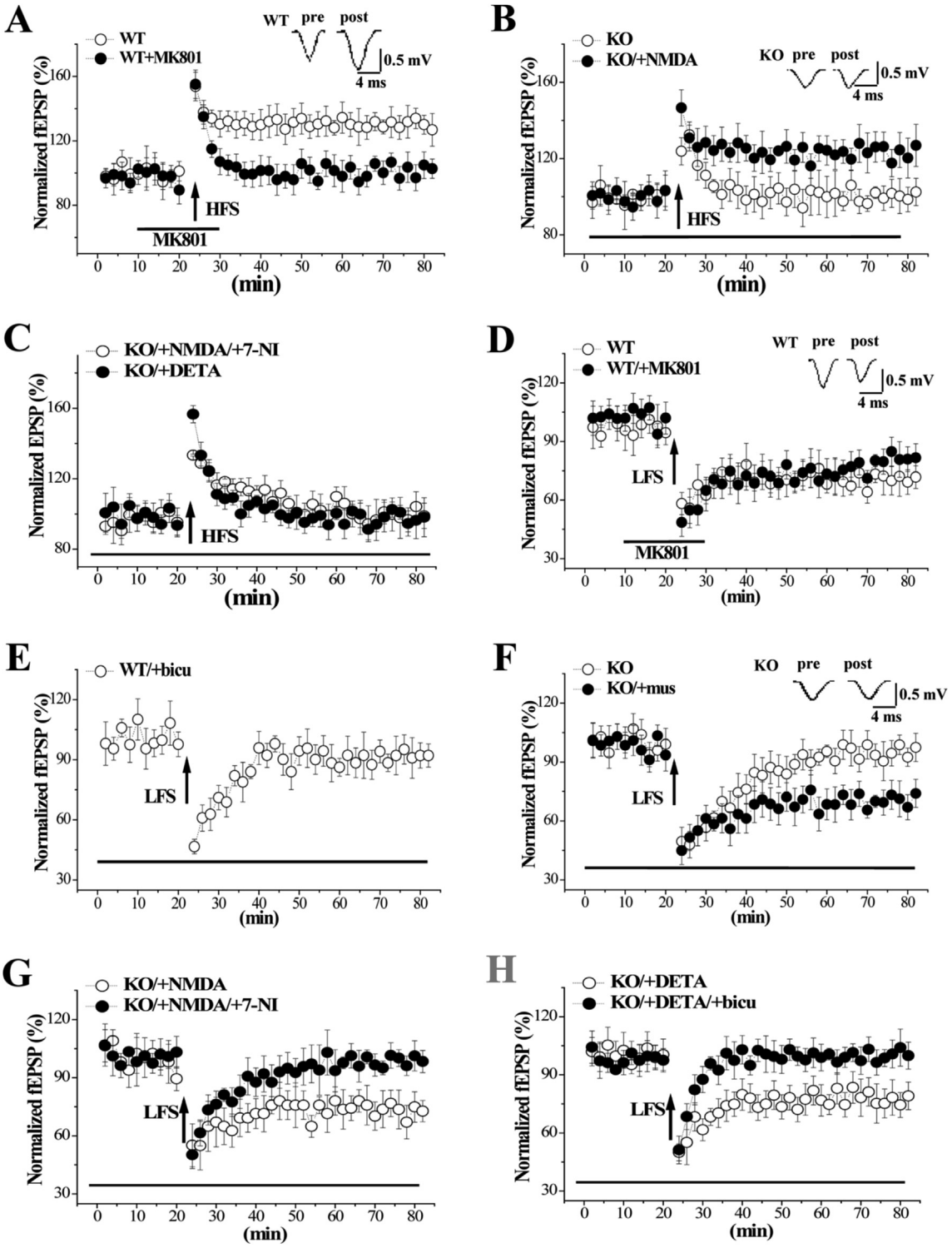

Fig. 5. Influence σ_1R deficiency on synaptic plasticity in BLA. (**A**) LTP induction by applying high-frequency stimulation (HFS) in WT mice. Each point represents the mean value of fEPSP slopes expressed as a percentage of baseline. (**B&C**) LTP induction in $\sigma_1R^{-/-}$ mice in the presence of NMDA, NMDA+7-NI or DETA/NO. (**D&E**) LTD induction by delivering low-frequency stimulation (LFS) in WT mice in the presence of MK801 or bicuculine (bicu). (**F**) LTD induction in $\sigma_1R^{-/-}$ mice in the presence of muscimol (mus). (**G&H**) LTD induction in $\sigma_1R^{-/-}$ mice in the presence of NMDA, NMDA+7-NI or DETA/NO. A solid arrow indicates when HFS or LFS was given. Black line indicates the duration of drugs applied. Representative sampling traces recorded at 5 min before HFS or LFS applied and at 60 min after HFS or LFS applied in WT slices (WT) or $\sigma_1R^{-/-}$ slices (KO).

through the decline of NR2B phosphorylation (Sha et al., 2013). Similarly, the level of NMDAr NR2B phosphorylation in BLA of $\sigma_1R^{-/-}$ mice was significantly reduced compared to WT mice. Pabba et al. (2014) reported that the activation of σ_1R increases the expression of NR2A and NR2B subunits in the rat hippocampus. The σ_1R and NMDAr may form a macromolecular complex, thus the activation of σ_1R can increase the association of σ_1R with NMDAr and trafficking of NMDAr to the cell surface. Although the NR2A and NR2B

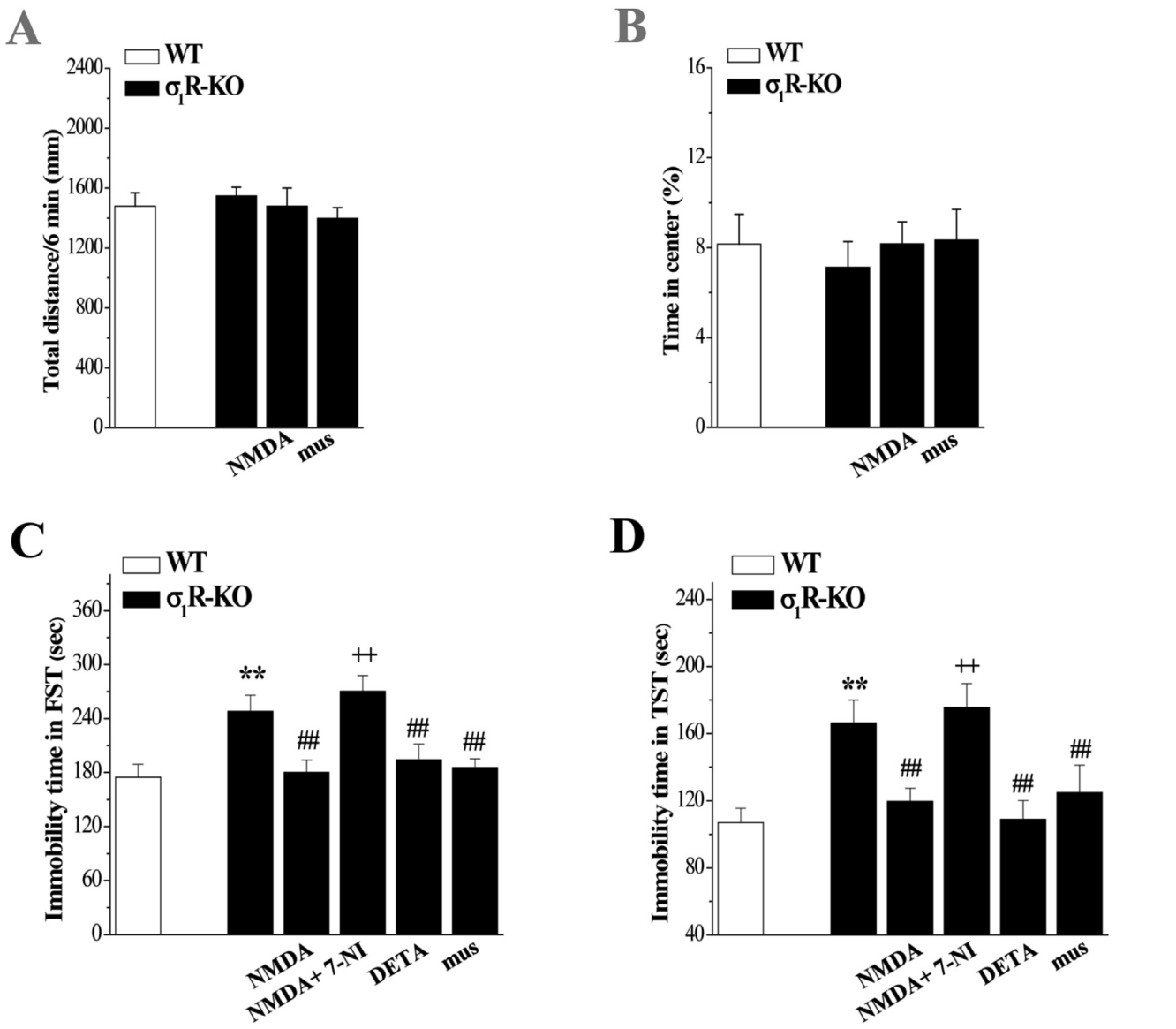

Fig. 6. Influence σ_1R deficiency on synaptic plasticity in BLA. (**A&B**) Bar graphs show the distance traveled in OFT and the time spent in the central partition of the arena in WT mice, $\sigma_1R^{-/-}$ mice and $\sigma_1R^{-/-}$ mice treated with BLA-injection of NMDA or muscimol (mus) for 3 days. (**C&D**) Bar graphs show the immobility time of FST and TST in WT mice and $\sigma_1R^{-/-}$ mice treated with BLA-injection of muscimol (mus), NMDA, NMDA+7-NI or DETA/NO for 3 days. $^{**}P < 0.01$ *vs*. WT mice; $\#\#P < 0.01$ *vs*. $\sigma_1R^{-/-}$ mice; $++P < 0.01$ *vs*. $\sigma_1R^{-/-}$ mice treated with NMDA (two-way ANOVA).

expression in BLA of $\sigma_1R^{-/-}$ mice did not differ significantly from WT mice, we cannot rule out the possibility that the σ_1R deficiency in BLA principal neurons affects the translocation of NMDAr to the cell surface. Furthermore, the path-application of NMDA in $\sigma_1R^{-/-}$ mice could correct the reduced fEPSP slopes and the increased PPF, although the acute application of MK801 in WT mice did not alter the fEPSP slopes and the PPF value. Therefore, the results give an indication that the σ_1R deficiency in BLA principal neurons reduces the presynaptic glutamate release *via* the dysfunction of post-synaptic NMDAr.

The PPI value reflects a $GABA_A$R-mediated inhibitory post-synaptic potential in BLA (Delaney and Sah, 2001). The PPI value in BLA of $\sigma_1R^{-/-}$ mice was larger than that in WT mice, which was corrected by the $GABA_A$R agonist muscimol. In addition, muscimol causes a larger decline of the fEPSP slopes in $\sigma_1R^{-/-}$ mice than that in WT mice. In contrast, the blockade of $GABA_A$R by bicuculine caused increases in the fEPSP slopes and the PPI value in WT mice, but not in $\sigma_1R^{-/-}$ mice. When the PPI value in $\sigma_1R^{-/-}$ mice was corrected by NMDA, the application of bicuculine could increase the PPI value. The expression of $GABA_A$R in BLA had no significant difference between WT mice and $\sigma_1R^{-/-}$ mice. The activity of $GABA_A$R in hippocampal pyramidal neurons of $\sigma_1R^{-/-}$ mice is not altered (Sha et al., 2013). Thus, it is highly likely that the σ_1R deficiency in BLA principal neurons causes the decline of $GABA_A$R-mediated inhibition probably through reducing NMDAr-mediated GABA release.

Several lines of evidence indicate that NO, as a retrograde messenger, diffuses rapidly to reach presynaptic terminals and enhances glutamate release (Micheva et al., 2003). The activation of NMDAr at glutamatergic synapses through increasing retrograde NO signaling enhances GABA release within the BLA (Lange et al., 2012). NO facilitates GABA release by activation of presynaptic guanylate cyclase. Our results showed that the application of DETA/NO could recover the presynaptic glutamate release and the

$GABA_AR$-mediated inhibition in BLA of $\sigma_1R^{-/-}$ mice. Moreover, the inhibition of nNOS abolished the effects of NMDA on the presynaptic glutamate release and $GABA_AR$-mediated inhibition in $\sigma_1R^{-/-}$ mice. Lange et al. (2012) observed the expression of nNOS in the BLA principal neurons. *The activation of σ_1R has been reported to enhance the expression of hippocampal nNOS in an NMDAr-dependent manner, which increases the production of NO* (Yang et al., 2011). *The nNOS expression and NO production are reduced in hippocampus of $\sigma_1R^{-/-}$ mice* (Zhang et al., 2016). *However, the nNOS expression in BLA of $\sigma_1R^{-/-}$ mice did not differ significantly from WT mice. The activity of nNOS in neuronal cells depends on the Ca^{2+} influx through NMDAr* (Hisatsune et al., 1997). *NO production highly depends on the coupling of nNOS to NMDAr or PSD-95* (Christopherson et al., 1999). *The levels of NMDAr, calmodulin and PSD-95 expression in BLA had no significant difference between WT mice and $\sigma_1R^{-/-}$ mice. Notably, the association of nNOS with PSD-95 was reduced, which was recovered by the application of NMDA. These results together with the NMDA-recovered NO production strongly suggested that the σ_1R deficiency reduces the activity of nNOS through reducing Ca^{2+}influx of NMDAr.* However, there are opposing reports describing that the activation of σ_1R disrupts the protein-protein interactions between NMDAr or PSD-95 and nNOS leading to lower levels of NO generation in hippocampal neurons (Pabba and Sibille, 2015). Low doses of σ_1R agonists enhance NMDAr function, while high doses of σ_1R agonists do not enhance NMDAr function (Liang and Wang, 1998). In addition, the σ_1R agonist reduces coupling of nNOS to PSD-95 in striatal neurons of global hypoxia-ischemia newborn piglets (Yang et al., 2010). Although this discrepancy is difficult to be reconciled in the present study, the contradictory effects of σ_1R on interactions of NMDAr and nNOS may arise from the difference in σ_1R expression and activity or experimental samplings and conditions.

In slices from fear-conditioned animals, HFS-induced LTP is attenuated, whereas LFS can elicit LTP, indicating that during maintenance of fear memory the mechanisms for LTP induction are altered (Schroeder and Shinnick-Gallagher, 2004). The induction of LTP or LTD in EC-BLA synapses was impaired in $\sigma_1R^{-/-}$ mice. Although the application of NMDA in $\sigma_1R^{-/-}$ mice rescued the induction of LTP and LTD, the application of DETA/NO only recovered the induction of LTD. In addition, the NMDA-rescued LTP induction in $\sigma_1R^{-/-}$ mice was sensitive to the inhibition of nNOS. Forebrain NR2B over-expression enhances LTP, but does not alter LTD (Duan et al., 2015). Mirante et al. (2014) observed that the NR2B antagonists did not affect the LTD induction in EC-BLA synapses. One simple explanation for the phenomenon is that the LTP induction in BLA depends on NMDAr activation, while the LTD induction is NMDAr-independent. The $GABA_AR$ antagonist blocked the induction of LTD in WT mice. The $GABA_AR$ agonist could recover the induction of LTD in $\sigma_1R^{-/-}$ mice. Thus, it is highly likely that the σ_1R deficiency in BLA impairs the induction of LTD through reducing $GABA_AR$-mediated inhibition.

In amygdale, LTP is involved specifically in the initial formation and/or stabilization of a learned fear response, whereas LTD may facilitate the suppression of fear responses during extinction (Dalton et al., 2012). The induction of LTD is associated with the extinction of fear memory (Hong et al., 2009; Kim et al., 2007; Park et al., 2012). The powerful GABAergic inhibitory circuit in BLA is very important in controlling motion and attention behavior (Martijena et al., 2002). The GABAergic system in amygdale networks appears to be involved in generating responses to fear-conditioned stimuli (Ehrlich et al., 2009) and is crucial for processes of fear extinction learning (Sangha et al., 2009). The NO system is known to play a prominent role in processes of fear generalization inhibition and fear extinction by modulating the GABAergic inhibitory circuit. The depression-like behaviors in $\sigma_1R^{-/-}$ mice could be improved by the BLA-injection of muscimol and DETA/NO. The BLA-injection of NMDA in $\sigma_1R^{-/-}$ mice was able to relieve the depression-like behaviors, which was abolished by 7-NI. By contrast, the time spent in the central partition during open-field test in $\sigma_1R^{-/-}$ mice did not differ from WT mice, which failed to be altered by the application of muscimol or NMDA. Thus, it is highly likely that the impairment of LTD rather than LTP induction in BLA of $\sigma_1R^{-/-}$ mice is responsible for the production of depressive-like phenotype.

In summary, the σ_1R deficiency in BLA principal neurons can cause the dysfunction of $GABA_AR$-mediated inhibition to impair the LTD induction, leading to the production of depressive-like phenotype. Results in the present study can help for understanding the molecular mechanisms underlying the production of depressive-like phenotype in $\sigma_1R^{-/-}$ mice and the antidepressant effects of the σ_1R agonists.

Contributors

Baofeng Zhang undertook the electrophysiological experiment and analysis. Ling Wang and Tingting Chen carried out the animal care and behavioral examinations. Sha Sha and Jun Wang undertook the western blotting and RT-PCR experiments. Ling Chen and Hang Xiao carried out the experimental design and the preparation of the manuscript.

Conflict of interest statement

The authors declare no competing financial conflict that could be construed as influencing the results or interpretation of the reported study.

Compliance with ethical standards

This article does not contain any studies with human participants or animals performed by any of the authors.

Acknowledgments

We thank Dr. Zorrilla (Neurosciences Graduate Program, University of California) for providing the sigma-1 receptor knockout mice. This study was supported by the National 973 Program (2014CB943303), the National Natural Science Foundation (81471157, 81671253, 31600835).

References

Alonso, G., Phan, V., Guillemain, I., Saunier, M., Legrand, A., Anoal, M., Maurice, T., 2000. Immunocytochemical localization of the sigma(1) receptor in the adult rat central nervous system. Neuroscience 97, 155–170.
Boehning, D., Snyder, S.H., 2003. Novel neural modulators. Annu. Rev. Neurosci. 26, 105–131.
Chae, S.Y., Lee, M., Kim, S.W., Bae, Y.H., 2004. Protection of insulin secreting cells from nitric oxide induced cellular damage by crosslinked hemoglobin. Biomaterials 25, 843–850.
Christopherson, K.S., Hillier, B.J., Lim, W.A., Bredt, D.S., 1999. PSD-95 assembles a ternary complex with the N-methyl-D-aspartic acid receptor and a bivalent neuronal NO synthase PDZ domain. J. Biol. Chem. 274, 27467–27473.
Dalton, G.L., Wu, D.C., Wang, Y.T., Floresco, S.B., Phillips, A.G., 2012. NMDA GluN2A and GluN2B receptors play separate roles in the induction of LTP and LTD in the amygdala and in the acquisition and extinction of conditioned fear. Neuropharmacology 62, 797–806.
Delaney, A.J., Sah, P., 2001. Pathway-specific targeting of GABA(A) receptor subtypes to somatic and dendritic synapses in the central amygdala. J. Neurophysiol. 86, 717–723.
Duan, Y., Zhou, S., Ma, J., Yin, P., Cao, X., 2015. Forebrain NR2B overexpression enhancing fear acquisition and long-term potentiation in the lateral amygdala. Eur. J. Neurosci. 42, 2214–2223.
Ehrlich, I., Humeau, Y., Grenier, F., Ciocchi, S., Herry, C., Luthi, A., 2009. Amygdala inhibitory circuits and the control of fear memory. Neuron 62, 757–771.
Etkin, A., Wager, T.D., 2007. Functional neuroimaging of anxiety: a meta-analysis of

emotional processing in PTSD, social anxiety disorder, and specific phobia. Am. J. Psychiatry 164, 1476–1488.
Fendt, M., Endres, T., Apfelbach, R., 2003. Temporary inactivation of the bed nucleus of the stria terminalis but not of the amygdala blocks freezing induced by trimethylthiazoline, a component of fox feces. J. Neurosci. 23, 23–28.
Goosens, K.A., Maren, S., 2002. Long-term potentiation as a substrate for memory: evidence from studies of amygdaloid plasticity and Pavlovian fear conditioning. Hippocampus 12, 592–599.
Hayashi, T., Su, T.P., 2004. Sigma-1 receptor ligands: potential in the treatment of neuropsychiatric disorders. CNS Drugs 18, 269–284.
Hisatsune, C., Umemori, H., Inoue, T., Michikawa, T., Kohda, K., Mikoshiba, K., Yamamoto, T., 1997. Phosphorylation-dependent regulation of N-methyl-D-aspartate receptors by calmodulin. J. Biol. Chem. 272, 20805–20810.
Hong, I., Song, B., Lee, S., Kim, J., Kim, J., Choi, S., 2009. Extinction of cued fear memory involves a distinct form of depotentiation at cortical input synapses onto the lateral amygdala. Eur. J. Neurosci. 30, 2089–2099.
Hu, Y., Wu, D.L., Luo, C.X., Zhu, L.J., Zhang, J., Wu, H.Y., Zhu, D.Y., 2012. Hippocampal nitric oxide contributes to sex difference in affective behaviors. Proc. Natl. Acad. Sci. U. S. A. 109, 14224–14229.
Isoardi, N.A., Martijena, I.D., Carrer, H.F., Molina, V.A., 2004. Increased fear learning coincides with neuronal dysinhibition and facilitated LTP in the basolateral amygdala following benzodiazepine withdrawal in rats. Neuropsychopharmacology 29, 1852–1864.
Kiedrowski, L., Costa, E., Wroblewski, J.T., 1992. In vitro interaction between cerebellar astrocytes and granule cells: a putative role for nitric oxide. Neurosci. Lett. 135, 59–61.
Kim, J., Lee, S., Park, K., Hong, I., Song, B., Son, G., Park, H., Kim, W.R., Park, E., Choe, H.K., Kim, H., Lee, C., Sun, W., Kim, K., Shin, K.S., Choi, S., 2007. Amygdala depotentiation and fear extinction. Proc. Natl. Acad. Sci. U. S. A. 104, 20955–20960.
Klenowski, P.M., Fogarty, M.J., Belmer, A., Noakes, P.G., Bellingham, M.C., Bartlett, S.E., 2015. Structural and functional characterization of dendritic arbors and GABAergic synaptic inputs on interneurons and principal cells in the rat basolateral amygdala. J. Neurophysiol. 114, 942–957.
Lange, M.D., Doengi, M., Lesting, J., Pape, H.C., Jungling, K., 2012. Heterosynaptic long-term potentiation at interneuron-principal neuron synapses in the amygdala requires nitric oxide signalling. J. Physiol. 590, 131–143.
Li, C., Rainnie, D.G., 2014. Bidirectional regulation of synaptic plasticity in the basolateral amygdala induced by the D1-like family of dopamine receptors and group II metabotropic glutamate receptors. J. Physiol. 592, 4329–4351.
Liang, X., Wang, R.Y., 1998. Biphasic modulatory action of the selective sigma receptor ligand SR 31742A on N-methyl-D-aspartate-induced neuronal responses in the frontal cortex. Brain Res. 807, 208–213.
Longone, P., di Michele, F., D'Agati, E., Romeo, E., Pasini, A., Rupprecht, R., 2011. Neurosteroids as neuromodulators in the treatment of anxiety disorders. Front. Endocrinol. (Lausanne) 2, 55.
Mameli, M., Carta, M., Partridge, L.D., Valenzuela, C.F., 2005. Neurosteroid-induced plasticity of immature synapses via retrograde modulation of presynaptic NMDA receptors. J. Neurosci. 25, 2285–2294.
Martijena, I.D., Rodriguez Manzanares, P.A., Lacerra, C., Molina, V.A., 2002. Gabaergic modulation of the stress response in frontal cortex and amygdala. Synapse 45, 86–94.
Martina, M., Turcotte, M.E., Halman, S., Bergeron, R., 2007. The sigma-1 receptor modulates NMDA receptor synaptic transmission and plasticity via SK channels in rat hippocampus. J. Physiol. 578, 143–157.
Maurice, T., Martin-Fardon, R., Romieu, P., Matsumoto, R.R., 2002. Sigma(1) (sigma(1)) receptor antagonists represent a new strategy against cocaine addiction and toxicity. Neurosci. Biobehav Rev. 26, 499–527.
Meyer, D.A., Carta, M., Partridge, L.D., Covey, D.F., Valenzuela, C.F., 2002. Neurosteroids enhance spontaneous glutamate release in hippocampal neurons. Possible role of metabotropic sigma1-like receptors. J. Biol. Chem. 277, 28725–28732.
Micheva, K.D., Buchanan, J., Holz, R.W., Smith, S.J., 2003. Retrograde regulation of synaptic vesicle endocytosis and recycling. Nat. Neurosci. 6, 925–932.
Mirante, O., Brandalise, F., Bohacek, J., Mansuy, I.M., 2014. Distinct molecular components for thalamic- and cortical-dependent plasticity in the lateral amygdala. Front. Mol. Neurosci. 7, 62.
Monnet, F.P., Maurice, T., 2006. The sigma1 protein as a target for the non-genomic effects of neuro(active)steroids: molecular, physiological, and behavioral aspects. J. Pharmacol. Sci. 100, 93–118.
Mtchedlishvili, Z., Kapur, J., 2003. A presynaptic action of the neurosteroid pregnenolone sulfate on GABAergic synaptic transmission. Mol. Pharmacol. 64, 857–864.
Pabba, M., Sibille, E., 2015. Sigma-1 and N-Methyl-d-Aspartate receptors: a partnership with beneficial outcomes. Mol. Neuropsychiatry 1, 47–51.
Pabba, M., Wong, A.Y., Ahlskog, N., Hristova, E., Biscaro, D., Nassrallah, W., Ngsee, J.K., Snyder, M., Beique, J.C., Bergeron, R., 2014. NMDA receptors are upregulated and trafficked to the plasma membrane after sigma-1 receptor activation in the rat hippocampus. J. Neurosci. 34, 11325–11338.
Paoletti, P., Bellone, C., Zhou, Q., 2013. NMDA receptor subunit diversity: impact on receptor properties, synaptic plasticity and disease. Nat. Rev. Neurosci. 14, 383–400.
Park, S., Lee, S., Kim, J., Choi, S., 2012. Ex vivo depotentiation of conditioning-induced potentiation at thalamic input synapses onto the lateral amygdala requires GluN2B-containing NMDA receptors. Neurosci. Lett. 530, 121–126.
Pose, I., Silveira, V., Damian, A., Higgie, R., Morales, F.R., 2014. Modulation of glycinergic synaptic transmission in the trigeminal and hypoglossal motor nuclei by the nitric oxide-cyclicGMP signaling pathway. Neuroscience 267, 177–186.
Sabino, V., Cottone, P., Parylak, S.L., Steardo, L., Zorrilla, E.P., 2009. Sigma-1 receptor knockout mice display a depressive-like phenotype. Behav. Brain Res. 198, 472–476.
Sanchez-Fernandez, C., Montilla-Garcia, A., Gonzalez-Cano, R., Nieto, F.R., Romero, L., Artacho-Cordon, A., Montes, R., Fernandez-Pastor, B., Merlos, M., Baeyens, J.M., Entrena, J.M., Cobos, E.J., 2014. Modulation of peripheral mu-opioid analgesia by sigma1 receptors. J. Pharmacol. Exp. Ther. 348, 32–45.
Sangha, S., Narayanan, R.T., Bergado-Acosta, J.R., Stork, O., Seidenbecher, T., Pape, H.C., 2009. Deficiency of the 65 kDa isoform of glutamic acid decarboxylase impairs extinction of cued but not contextual fear memory. J. Neurosci. 29, 15713–15720.
Schafe, G.E., Bauer, E.P., Rosis, S., Farb, C.R., Rodrigues, S.M., LeDoux, J.E., 2005. Memory consolidation of Pavlovian fear conditioning requires nitric oxide signaling in the lateral amygdala. Eur. J. Neurosci. 22, 201–211.
Schiess, A.R., Partridge, L.D., 2005. Pregnenolone sulfate acts through a G-protein-coupled sigma1-like receptor to enhance short term facilitation in adult hippocampal neurons. Eur. J. Pharmacol. 518, 22–29.
Schroeder, B.W., Shinnick-Gallagher, P., 2004. Fear memories induce a switch in stimulus response and signaling mechanisms for long-term potentiation in the lateral amygdala. Eur. J. Neurosci. 20, 549–556.
Senn, V., Wolff, S.B., Herry, C., Grenier, F., Ehrlich, I., Grundemann, J., Fadok, J.P., Muller, C., Letzkus, J.J., Luthi, A., 2014. Long-range connectivity defines behavioral specificity of amygdala neurons. Neuron 81, 428–437.
Sha, S., Hong, J., Qu, W.J., Lu, Z.H., Li, L., Yu, W.F., Chen, L., 2015. Sex-related neurogenesis decrease in hippocampal dentate gyrus with depressive-like behaviors in sigma-1 receptor knockout mice. Eur. Neuropsychopharmacol. 25, 1275–1286.
Sha, S., Qu, W.J., Li, L., Lu, Z.H., Chen, L., Yu, W.F., Chen, L., 2013. Sigma-1 receptor knockout impairs neurogenesis in dentate gyrus of adult hippocampus via down-regulation of NMDA receptors. CNS Neurosci. Ther. 19, 705–713.
Shaban, H., Humeau, Y., Herry, C., Cassasus, G., Shigemoto, R., Ciocchi, S., Barbieri, S., van der Putten, H., Kaupmann, K., Bettler, B., Luthi, A., 2006. Generalization of amygdala LTP and conditioned fear in the absence of presynaptic inhibition. Nat. Neurosci. 9, 1028–1035.
Spampanato, J., Polepalli, J., Sah, P., 2011. Interneurons in the basolateral amygdala. Neuropharmacology 60, 765–773.
Urani, A., Roman, F.J., Phan, V.L., Su, T.P., Maurice, T., 2001. The antidepressant-like effect induced by sigma(1)-receptor agonists and neuroactive steroids in mice submitted to the forced swimming test. J. Pharmacol. Exp. Ther. 298, 1269–1279.
Wright, B.T., Gluszek, C.F., Heldt, S.A., 2014. The effects of repeated zolpidem treatment on tolerance, withdrawal-like symptoms, and GABAA receptor mRNAs profile expression in mice: comparison with diazepam. Psychopharmacol. Berl. 231, 2967–2979.
Yang, R., Zhou, R., Chen, L., Cai, W., Tomimoto, H., Sokabe, M., Chen, L., 2011. Pregnenolone sulfate enhances survival of adult-generated hippocampal granule cells via sustained presynaptic potentiation. Neuropharmacology 60, 529–541.
Yang, Z.J., Carter, E.L., Torbey, M.T., Martin, L.J., Koehler, R.C., 2010. Sigma receptor ligand 4-phenyl-1-(4-phenylbutyl)-piperidine modulates neuronal nitric oxide synthase/postsynaptic density-95 coupling mechanisms and protects against neonatal ischemic degeneration of striatal neurons. Exp. Neurol. 221, 166–174.
Zhang, S., Hong, J., Zhang, T., Wu, J., Chen, L., 2016. Activation of Sigma-1 receptor alleviates postpartum estrogen withdrawal-induced "Depression" through restoring hippocampal nNOS-NO-CREB activities in mice. Mol. Neurobiol. http://dx.doi.org/10.1007/s12035-016-9872-8. PMID: 27032391.
Zhou, L., Chen, T., Li, G., Wu, C., Wang, C., Li, L., Sha, S., Chen, L., Liu, G., Chen, L., 2016. Activation of PPARgamma ameliorates spatial cognitive deficits through restoring expression of AMPA receptors in seipin knock-out mice. J. Neurosci. 36, 1242–1253.
Zhou, Q.G., Hu, Y., Wu, D.L., Zhu, L.J., Chen, C., Jin, X., Luo, C.X., Wu, H.Y., Zhang, J., Zhu, D.Y., 2011a. Hippocampal telomerase is involved in the modulation of depressive behaviors. J. Neurosci. 31, 12258–12269.
Zhou, R., Bai, Y., Yang, R., Zhu, Y., Chi, X., Li, L., Chen, L., Sokabe, M., Chen, L., 2011b. Abnormal synaptic plasticity in basolateral amygdala may account for hyperactivity and attention-deficit in male rat exposed perinatally to low-dose bisphenol-A. Neuropharmacology 60, 789–798.